

11-27-2009

Formation of Compositionally Abrupt Axial Heterojunctions in Silicon-Germanium Nanowires

C Y. Wen

Purdue University - Main Campus

M C. Reuter

IBM Corp

J Bruley

IBM Corp

J Tersoff

IBM Corp

S Kodambaka

University of California - Los Angeles

See next page for additional authors

Follow this and additional works at: <http://docs.lib.purdue.edu/nanopub>

 Part of the [Nanoscience and Nanotechnology Commons](#)

Wen, C Y.; Reuter, M C.; Bruley, J; Tersoff, J; Kodambaka, S; Stach, E A.; and Ross, F M., "Formation of Compositionally Abrupt Axial Heterojunctions in Silicon-Germanium Nanowires" (2009). *Birck and NCN Publications*. Paper 568.
<http://docs.lib.purdue.edu/nanopub/568>

This document has been made available through Purdue e-Pubs, a service of the Purdue University Libraries. Please contact epubs@purdue.edu for additional information.

Authors

C Y. Wen, M C. Reuter, J Bruley, J Tersoff, S Kodambaka, E A. Stach, and F M. Ross

the growing crystal (4, 15), physical entrapment can occur for a wide range of organic material. This work suggests an approach for modifying the internal structures of crystals and synthesizing single-crystal composites with large, potentially accessible, internal surface areas. Potential uses for the gel method include the preparation of materials that require both high crystallinity and high surface areas, such as photovoltaic materials (31).

References and Notes

1. Y. Politi, T. Arad, E. Klein, S. Weiner, L. Addadi, *Science* **306**, 1161 (2004).
2. J. Aizenberg, D. A. Muller, J. L. Grazul, D. R. Hamann, *Science* **299**, 1205 (2003).
3. J. Aizenberg, A. Tkachenko, S. Weiner, L. Addadi, G. Hendler, *Nature* **412**, 819 (2001).
4. J. Aizenberg, J. Hanson, T. F. Koetzle, S. Weiner, L. Addadi, *J. Am. Chem. Soc.* **119**, 881 (1997).
5. J. S. Robach, S. R. Stock, A. Veis, *J. Struct. Biol.* **151**, 18 (2005).
6. F. Nudelman, H. H. Chen, H. A. Goldberg, S. Weiner, L. Addadi, *Faraday Discuss.* **136**, 9 (2007).
7. A. Berman et al., *Science* **259**, 776 (1993).

8. A. Berman et al., *Science* **250**, 664 (1990).
9. B. Pokroy et al., *J. Struct. Biol.* **155**, 96 (2006).
10. H. Y. Li, L. A. Estroff, *J. Am. Chem. Soc.* **129**, 5480 (2007).
11. H. Y. Li, L. A. Estroff, *CrystEngComm* **9**, 1153 (2007).
12. S. Sindhu et al., *Adv. Funct. Mater.* **17**, 1698 (2007).
13. R. J. Park, F. C. Meldrum, *Adv. Mater.* **14**, 1167 (2002).
14. C. Li, L. M. Qi, *Angew. Chem. Int. Ed.* **47**, 2388 (2008).
15. A. N. Kulak et al., *J. Am. Chem. Soc.* **129**, 3729 (2007).
16. Materials and methods are available as supporting material on Science Online.
17. J. K. Hyun, P. Ercius, D. A. Muller, *Ultramicroscopy* **109**, 1 (2008).
18. P. A. Midgley, M. Weyland, *Ultramicroscopy* **96**, 413 (2003).
19. H. Y. Li, L. A. Estroff, *Adv. Mater.* **21**, 470 (2009).
20. J. J. De Yoreo, P. M. Dove, *Science* **306**, 1301 (2004).
21. C. A. Orme et al., *Nature* **411**, 775 (2001).
22. S. Mann et al., *Science* **261**, 1286 (1993).
23. L. A. Estroff, C. D. Incarvito, A. D. Hamilton, *J. Am. Chem. Soc.* **126**, 2 (2004).
24. N. Sommerdijk, G. de With, *Chem. Rev.* **108**, 4499 (2008).
25. E. M. Pouget et al., *Science* **323**, 1455 (2009).
26. R. Q. Song, A. W. Xu, M. Antonietti, H. Colfen, *Angew. Chem. Int. Ed.* **48**, 395 (2009).
27. J. Aizenberg, A. J. Black, G. M. Whitesides, *Nature* **398**, 495 (1999).

28. A. M. Travaille et al., *J. Am. Chem. Soc.* **125**, 11571 (2003).
29. D. Volkmer, M. Fricke, C. Agena, J. Mattay, *J. Mater. Chem.* **14**, 2249 (2004).
30. D. X. Du, D. J. Srolovitz, M. E. Coltrin, C. C. Mitchell, *Phys. Rev. Lett.* **95**, 155503 (2005).
31. I. Gur, N. A. Fromer, M. L. Geier, A. P. Alivisatos, *Science* **310**, 462 (2005).
32. L.A.E. acknowledges partial support from NSF (DMR 0845212), the J. D. Watson Investigator Program (New York State Office of Science, Technology, and Academic Research contract C050017), and the Cornell Center for Materials Research (CCMR), a Materials Research Science and Engineering Center of NSF (DMR 0520404). H.L.X. and D.M. acknowledge the Semiconductor Research Corporation and CCMR. Particular acknowledgement is made of the use of the EM and polymer characterization facilities of CCMR.

Supporting Online Material

www.sciencemag.org/cgi/content/full/326/5957/1244/DC1
Materials and Methods

Figs. S1 to S8

References

Movies S1 to S4

2 July 2009; accepted 14 October 2009

10.1126/science.1178583

Formation of Compositionally Abrupt Axial Heterojunctions in Silicon-Germanium Nanowires

C.-Y. Wen,¹ M. C. Reuter,² J. Bruley,² J. Tersoff,² S. Kodambaka,³ E. A. Stach,¹ F. M. Ross^{2*}

We have formed compositionally abrupt interfaces in silicon-germanium (Si-Ge) and Si-SiGe heterostructure nanowires by using solid aluminum-gold alloy catalyst particles rather than the conventional liquid semiconductor-metal eutectic droplets. We demonstrated single interfaces that are defect-free and close to atomically abrupt, as well as quantum dots (i.e., Ge layers tens of atomic planes thick) embedded within Si wires. Real-time imaging of growth kinetics reveals that a low solubility of Si and Ge in the solid particle accounts for the interfacial abruptness. Solid catalysts that can form functional group IV nanowire-based structures may yield an extended range of electronic applications.

The most exciting applications of semiconductor nanowires—for electronic devices as well as for fundamental research into transport phenomena—do not come from compositionally uniform structures, but from heterostructure nanowires in which the composition changes along the length of the wire. These axial heterostructures are particularly important for applications such as tunnel field-effect transistors and thermoelectric devices (1–4). A prerequisite for optimal device performance in these applications is the formation of compositionally abrupt and structurally perfect junctions (5, 6). The relative ease of forming abrupt, defect-free

junctions in group III-V nanowires composed of materials pairs such as InAs-InP has been key to realizing devices such as double-barrier resonant tunneling devices and single-electron transistors (3, 7–9). Yet abrupt interfaces have not been formed in group IV nanowires, creating a severe constraint on the use of group IV materials in nanowire applications. This is thought to be due to the fundamental nature of the process by which the nanowires grow.

Si and Ge nanowires are commonly fabricated using the vapor-liquid-solid (VLS) mechanism (10). In this method, droplets of a liquid catalyst are formed on a substrate via eutectic reaction between the semiconductor and a metal, typically gold, above the eutectic temperature T_{eu} . A vapor-phase semiconductor reactant, such as silane or germane, is then introduced and is preferentially dissociated by the liquid catalyst and dissolved into the liquid. Once the concentration of semiconductor atoms in the catalyst reaches

supersaturation, the semiconductor precipitates at the liquid-substrate interface. Nanowires then grow as material is added in a layer-by-layer fashion at the liquid-solid interface. To create a junction between two different semiconductors, the vapor-phase reactants are modulated during growth. This, of course, requires a catalyst suitable for the growth of both components under compatible conditions.

Group IV heterostructure nanowires containing dislocation-free Si and SiGe segments have been grown successfully using this approach (11, 12). However, the interfaces are diffuse, showing a broad composition gradient. A similar broadening of Si-Ge interfaces has also been seen for “MBE-grown” nanowires, where the same Au starting material is used but the Si and Ge are supplied by molecular beam epitaxy (13, 14). Theoretical modeling and experimental investigation (12, 15) suggest that this interface diffuseness is due to a “reservoir effect.” The catalytic droplet contains a large amount of the growth species; AuSi and AuGe contain more than 20 atomic percent of Si or Ge, respectively. This means that when the reactant supply is switched, say from silane to germane, the droplet must be depleted of Si before pure Ge can be deposited. It is found (12) that the length of the compositionally graded region scales with wire diameter, as expected from the modeling (12, 15). Because interface diffuseness is due to the high solubility of Si and Ge in the catalyst, it cannot be avoided with the usual liquid semiconductor-metal catalysts. However, in solid metal catalysts the solubility of Si or Ge can be very low, so that rapid depletion of each material would be expected. Our approach to an abrupt interface in a nanowire junction structure exploits the potential of solid catalysts and uses the vapor-solid-solid (VSS) growth mechanism.

¹School of Materials Engineering and Birk Nanotechnology Center, Purdue University, West Lafayette, IN 47907, USA.

²IBM T. J. Watson Research Center, Yorktown Heights, NY 10598, USA. ³Department of Materials Science and Engineering, University of California, Los Angeles, CA 90095, USA.

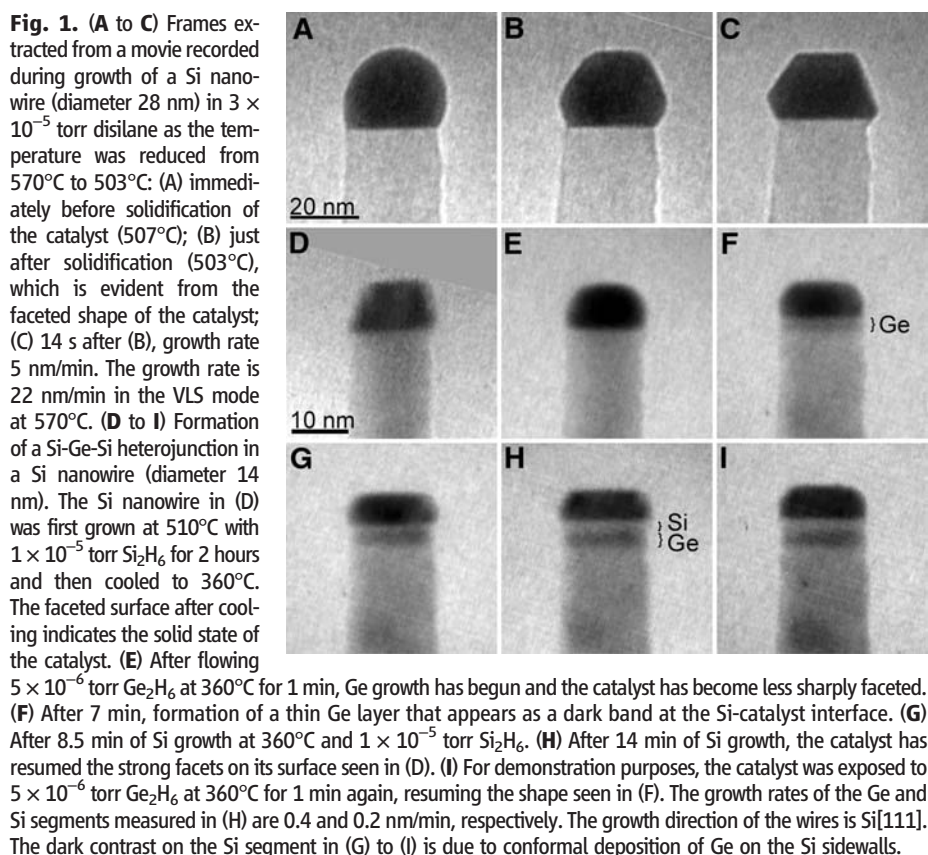
*To whom correspondence should be addressed. E-mail: fmross@us.ibm.com

Several solid catalysts have been used to grow Si and Ge nanowires (16–22). We ruled out the use of metal silicides or germanides (18–22) for our purpose, because of possible reservoir effects due to transformations between silicide and germanide during formation of the heterostructure. Solid Au catalyzes Ge wire growth (16), but because the reaction must be carried out below T_{eu} (~360°C for both Si and Ge), VSS growth is impractically slow for conventional Si and Ge reactants. Aluminum, which is of interest for photovoltaic nanowire applications because of its electronic properties in Si (23), has a higher T_{eu} (577°C) but slow Si wire growth kinetics (17, 24). To realize efficient heterojunction nanowire growth, we sought a solid catalyst that is suitable for both Si and Ge and that can provide practical growth rates. To this end, we added Al to Au catalysts (i) to raise the eutectic temperature with Si or Ge, and hence the nanowire growth temperature and growth rate under VSS, while (ii) maintaining the high reactivity known for Au. The ternary phase diagrams of Al-Au-Si and Al-Au-Ge have not been determined experimentally, but theoretical calculations predict a eutectic temperature of Si with one of the intermetallic compounds, AlAu_2 , of 487°C (25). Because of the similarity in physical properties between Si and Ge, we might expect Ge to have a similar T_{eu} with AlAu_2 .

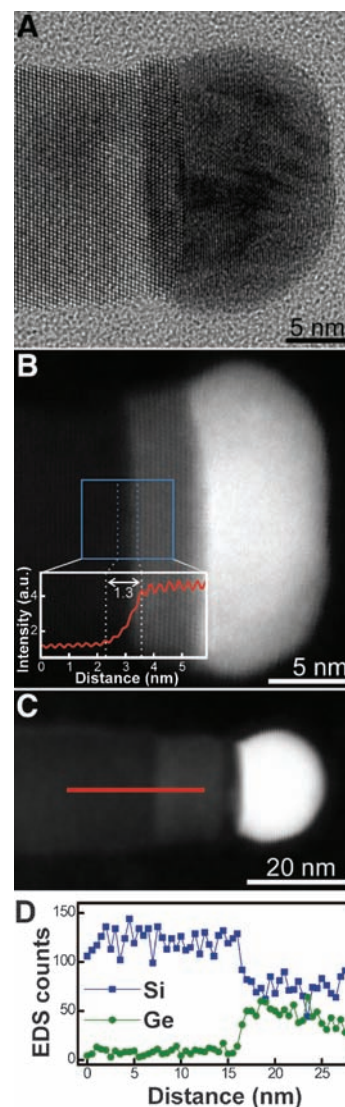
Growth experiments were conducted in a transmission electron microscope (TEM) (26), because real-time observations proved useful in providing structural information during growth

as well as in tuning the growth parameters (27). The catalyst was prepared by thermally evaporating Au and Al sequentially with an atomic ratio of 2:1. Two growth modes are possible in this system, the faster VLS and the slower VSS, with T_{eu} around the expected value (Fig. 1, A to C). Figure 1, D to I, shows the growth sequence of a Si-Ge-Si heterostructure as it forms in a single nanowire. We first grew long Si nanowires in the VLS mode and then cooled them below T_{eu} to obtain the VSS mode (Fig. 1D). Subsequent modulation in the gas source produced the junction segments effectively (Fig. 1, E to I). Under these imaging conditions, Ge exhibits darker contrast, and the sharp change between the narrow Ge layer (or “quantum dot”) and the surrounding Si hints at compositionally abrupt interfaces. The VSS growth rates for Ge and Si are slower than the rapid VLS Si nanowire growth but are still practical for the purpose of growing the heterostructure.

We quantify the structural perfection and the compositional abruptness of the Si-Ge interface in Fig. 2, where we have simplified the structure by growing only a Ge layer on the tip of a Si nanowire in order to avoid ambiguity in analysis due to overlay of materials on wire sidewalls. The analysis in Fig. 2 was obtained after (rather than during) growth, allowing the use of microscopes with analytical capabilities and higher spatial resolution but requiring the sample to be exposed to air (26). In Fig. 2A we see that the interface exhibits a single crystalline structure



without obvious crystal defects such as dislocations. High-angle annular dark-field scanning TEM (HAADF-STEM; Fig. 2B) confirms the



without obvious crystal defects such as dislocations. High-angle annular dark-field scanning TEM (HAADF-STEM; Fig. 2B) confirms the

presence of a compositionally uniform Ge segment on the Si nanowire. The average intensity profile (Fig. 2B, inset) shows a rather narrow transition (~ 1.3 nm) at the interface. STEM energy dispersive x-ray spectroscopy (EDS) line profiles (26) (Fig. 2D and fig. S1) show that the composition transition occurs in less than 2 nm, in agreement with the HAADF analysis. EDS maps (Fig. 3) confirm the uniform Ge distribution in the Ge layer; they show that there is no Si or Ge in the bulk of the catalyst and no Si in the Ge (at the detection limit, $\sim 2\%$). These results can be compared with the diffuseness of interfaces measured (using similar techniques) during a comprehensive study of Si-SiGe heterostructures grown using liquid catalysts (12); wires of the diameter shown in Fig. 2 were found to have diffuse interfaces with compositional widths on the order of 18 to 24 nm.

Apart from the reservoir effect, other factors may affect the measured interface abruptness, including Si-Ge interdiffusion at the growth

temperature and broadening of the STEM probe. A previous study of Ge self-diffusion in $\text{Si}_{1-x}\text{Ge}_x$ ($0 \leq x \leq 0.5$) under various strain conditions suggested that Si-Ge interdiffusion at the nanowire growth temperature should be slow enough to be negligible over our growth times (28). Electron beam broadening, however, does cause a noticeable error in determining interface abruptness (29). Using Goldstein's single-scattering equation (29), we estimate a beam broadening of 0.3 nm in Si and 0.6 nm in Ge (using a wire thickness of 20 nm and an electron energy of 300 keV). Adding these effects to the original 0.5-nm probe, an atomically abrupt interface should appear with a width of ~ 1 nm. In other words, the compositional width of our Si-Ge interface is probably less than that shown in the profiles in Figs. 2 and 3 and fig. S1, and may be below 1 nm. Any physical roughness (nonplanarity of the interface) would also contribute to the measured interface abruptness. We cannot completely rule out the possibility that some Si could remain in the catalyst, but any reservoir effect must be small, as we do not see a measurable difference between the widths of the interfaces in wires 20 nm and 10 nm in diameter (26) (fig. S1). Because Ge and Si are not detectable in the catalyst, their solubility is low, fully supporting the advantage of using a solid catalyst to reduce the reservoir effect.

During VSS growth, ledge nucleation and flow at the catalyst-wire interface is evident (fig. S2) and is expected in VSS systems (20). Here, by measuring the kinetics of individual ledge motion, we found evidence to support a solubility of Si and Ge in the solid catalyst that is low relative to the solubility in liquid Au eutectic droplets. During VSS growth of Si, we found that ledges nucleate only a short time after a previous ledge has finished propagating (fig. S2). In contrast, for VLS growth at the same overall growth rates, we observed quite different ledge flow kinetics (fig. S3): long "incubation times" (several seconds) between ledges, followed by very rapid ledge propagation at a rate too fast to measure. In VLS, it is not surprising that substantial excess Si or Ge is needed to raise the chemical potential high enough to nucleate a ledge. This excess provides a large driving force and supply for the subsequent rapid motion. For VSS, the short incubation time suggests that even a tiny amount of excess Si raises the chemical potential enough to nucleate a ledge, consistent with low solubility. In that case, the excess Si would be too small to drive the ledge very far, and subsequent motion would then be supply-limited, depending directly on the incoming flux.

The fact that ledge motion depends directly on the incoming flux is particularly relevant to the growth of SiGe alloy segments in nanowires. When growing alloy segments from liquid eutectic droplets, the composition profiles at Si-SiGe interfaces are found to be curved (12); in other words, the central region of the wire switches composition at a different rate relative to regions

nearer the wire surface. This effect is thought to arise because, although the growth interface remains planar, the incorporation ratio of Si and Ge changes as a result of varying strain (12). Here, we expect such effects to be avoided or minimized because of the direct dependence of the deposited composition on the gas supply. Indeed, SiGe segments grown from solid catalysts (Fig. 2, C and D) by flowing disilane and digermane simultaneously show abrupt and planar Si-SiGe interfaces (< 2 nm wide) and a uniform composition within the SiGe segment.

The following are some practical considerations for extending the technique of using a solid catalyst with low group IV solubility to create abrupt heterointerfaces in nanowires.

1) We have mentioned the need for a relatively high eutectic temperature, so that the VSS growth mode can be obtained at temperatures high enough to achieve reasonably fast growth rates. However, it is also useful to be able to access the VLS growth mode when needed, by means of a small increase in temperature. This was shown in Fig. 1 where the VLS mode was used to expedite Si nanowire growth, forming wire segments hundreds of nanometers in length, after which the sample was cooled to obtain VSS Si growth before forming Si-Ge interfaces or quantum dots.

2) To form wires consistently with a particular morphology (i.e., a well-defined cross-sectional shape and growth direction and no kinking), we suggest that it is advantageous to have a strong orientation relationship between the solid catalyst crystal and the wire. For the majority of wires, the AlAu_2 catalyst we have used here exhibits a large top facet and a flat shape, and this orientation forms wires that are generally uninked.

3) The solid catalyst must be able to grow both Si and Ge segments without changes in its shape, because shape changes could alter the wire diameter.

It is our belief that other solid materials that catalyze Si and Ge wire growth should be useful in forming abrupt heterointerfaces, provided that they satisfy the requirements above in terms of eutectic temperature, the existence of a preferred orientation relationship, and minimal changes in shape between growing Si and growing Ge.

Our results show that axial Si-Ge nanowire heterostructures in which the composition is modulated at the nanometer scale can be realized by using an AlAu alloy catalyst operating via the VSS growth mechanism. This method provides control over compositional modulation that is superior to that possible with the use of conventional AuSi-AuGe liquid catalysts. The key to achieving this control is twofold: The solid state of the catalyst leads to a low solubility of Si or Ge and avoids the reservoir effect that accounts for the smearing of compositional changes, and the tuning of the eutectic temperature allows rapid growth with a VLS mode to form long uniform segments, as well as VSS growth at a slower yet practical rate for nanoscale control of interfaces,

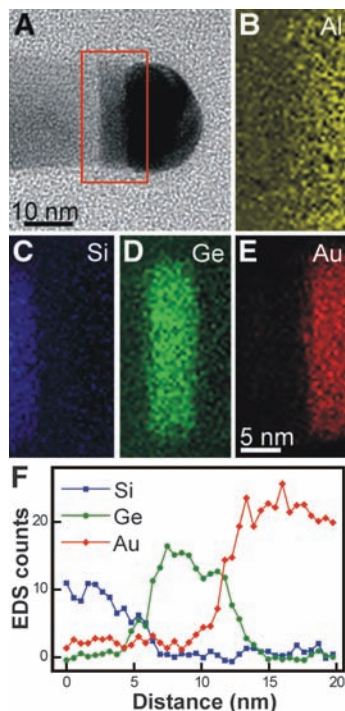


Fig. 3. Composition analysis of a Si-Ge heterojunction nanowire grown under the conditions of Fig. 2A. (A to E) Bright-field TEM image (A) and false-color STEM EDS elemental maps (B to E) of Al, Si, Ge, and Au in the region [defined in (A)] of the junction in a nanowire 22 nm in diameter. The catalyst is surrounded by an amorphous shell, 2 nm thick, that forms after air exposure. The stronger Al signal in this region and the difference in interface diffuseness between the Al and Au maps suggests that the shell is aluminum oxide, consistent with the results of oxidation of AlAu alloys described in (30). (F) Line profile of the EDS intensities extracted from the elemental maps of Si, Ge, and Au. The intensity is averaged over a 3-nm strip along the midpoint of the wire.

quantum dots, and barriers. We believe that this approach should apply to solid catalyst materials other than AlAu alloys, and indeed to wire materials other than Si and Ge, provided that the catalyst and wire material satisfy requirements for eutectic temperature, orientation, and stability. We speculate that a solid catalyst could be similarly advantageous in forming abrupt doping profiles, such as are required for high-subthreshold slope devices such as tunnel and avalanche field-effect transistors. More generally, Si and Ge device fabrication that requires sophisticated control of composition and structure can be addressed using this approach.

References and Notes

1. M. S. Gudixsen, L. J. Lauhon, J. Wang, D. C. Smith, C. M. Lieber, *Nature* **415**, 617 (2002).
2. C. Yang, Z. Zhong, C. M. Lieber, *Science* **310**, 1304 (2005).
3. M. T. Björk *et al.*, *Nano Lett.* **4**, 1621 (2004).

4. D. Li, Y. Wu, R. Fan, P. Yang, A. Majumdar, *Appl. Phys. Lett.* **83**, 3186 (2003).
5. C. M. Lieber, *Nano Lett.* **2**, 81 (2002).
6. L. Samuelson *et al.*, *Physica E* **25**, 313 (2004).
7. M. T. Björk *et al.*, *Appl. Phys. Lett.* **81**, 4458 (2002).
8. M. T. Björk *et al.*, *Nano Lett.* **2**, 87 (2002).
9. C. Thelander *et al.*, *Appl. Phys. Lett.* **83**, 2052 (2003).
10. R. S. Wagner, W. C. Ellis, *Appl. Phys. Lett.* **4**, 89 (1964).
11. Y. Wu, R. Fan, P. Yang, *Nano Lett.* **2**, 83 (2002).
12. T. E. Clark *et al.*, *Nano Lett.* **8**, 1246 (2008).
13. N. D. Zakharov *et al.*, *J. Cryst. Growth* **290**, 6 (2006).
14. R. Dujardin *et al.*, *Appl. Phys. Lett.* **89**, 153129 (2006).
15. N. Li, T. Y. Tan, U. Gösele, *Appl. Phys. A* **90**, 591 (2008).
16. S. Kodambaka, J. Tersoff, M. C. Reuter, F. M. Ross, *Science* **316**, 729 (2007).
17. Y. Wang, V. Schmidt, S. Senz, U. Gösele, *Nat. Nanotechnol.* **1**, 186 (2006).
18. T. I. Kamins, R. S. Williams, D. P. Basile, T. Hesjedal, J. S. Harris, *J. Appl. Phys.* **89**, 1008 (2001).
19. J. Arbiol, B. Kalache, P. Roca i Cabarrocas, J. R. Morante, A. Fontcuberta i Morral, *Nanotechnology* **18**, 305606 (2007).
20. S. Hofmann *et al.*, *Nat. Mater.* **7**, 372 (2008).
21. K. Kang *et al.*, *Adv. Mater.* **20**, 4684 (2008).
22. J. L. Lensch-Falk, E. R. Hemesath, F. J. Lopez, L. J. Lauhon, *J. Am. Chem. Soc.* **129**, 10670 (2007).

23. J. R. Davis *et al.*, *IEEE Trans. Electron. Dev.* **27**, 677 (1980).
24. B. A. Wacaser *et al.*, *Nano Lett.* **9**, 3296 (2009).
25. M. Hoch, *J. Alloy. Comp.* **220**, 27 (1995).
26. See supporting material on Science Online.
27. F. M. Ross, J. Tersoff, M. C. Reuter, *Phys. Rev. Lett.* **95**, 146104 (2005).
28. N. R. Zangenberg, J. Lundsgaard Hansen, J. Fage-Pedersen, A. Nylandsted Larsen, *Phys. Rev. Lett.* **87**, 125901 (2001).
29. D. C. Joy, A. D. Romig, J. I. Goldstein, *Principles of Analytical Electron Microscopy* (Plenum, New York, 1986).
30. H. Piao, M. Suominen Fuller, D. Miller, N. S. McIntyre, *Appl. Surf. Sci.* **187**, 266 (2002).
31. We acknowledge A. Ellis and L. Gignac of IBM for their assistance with experimental aspects of this work. Supported by NSF grants DMR-0606395 and DMR-0907483 and by the University of California Energy Institute.

Supporting Online Material

www.sciencemag.org/cgi/content/full/326/5957/1247/DC1

Materials and Methods

Figs. S1 to S3

References

26 August 2009; accepted 29 September 2009

10.1126/science.1178606

Selective Phenol Hydrogenation to Cyclohexanone Over a Dual Supported Pd–Lewis Acid Catalyst

Huizhen Liu, Tao Jiang,* Buxing Han,* Shuguang Liang, Yinxi Zhou

Cyclohexanone is an industrially important intermediate in the synthesis of materials such as nylon, but preparing it efficiently through direct hydrogenation of phenol is hindered by over-reduction to cyclohexanol. Here we report that a previously unappreciated combination of two common commercial catalysts—nanoparticulate palladium (supported on carbon, alumina, or NaY zeolite) and a Lewis acid such as AlCl₃—synergistically promotes this reaction. Conversion exceeding 99.9% was achieved with >99.9% selectivity within 7 hours at 1.0-megapascal hydrogen pressure and 50°C. The reaction was accelerated at higher temperature or in a compressed CO₂ solvent medium. Preliminary kinetic and spectroscopic studies suggest that the Lewis acid sequentially enhances the hydrogenation of phenol to cyclohexanone and then inhibits further hydrogenation of the ketone.

Cyclohexanone is a key raw material in the synthesis of many useful chemical intermediates, such as caprolactam for nylon 6 and adipic acid for nylon 66 (1, 2). The industrial production of cyclohexanone typically involves either the oxidation of cyclohexane (3, 4) or the hydrogenation of phenol. The former route requires high temperature and generates byproducts such as cyclohexanol and organic acids that complicate purification, and the yield of cyclohexanone is usually low. The phenol hydrogenation route is undertaken through either two-step or one-step processes. In the two-step procedure, phenol is first hydrogenated to cyclohexanol, which in turn is dehydrogenated to cyclohexanone at high temperature. The one-step selective hydrogenation of phenol to cyclohexanone is advantageous from an efficiency standpoint, and

the reaction can be conducted in either the gas phase or liquid phase. The gas-phase phenol hydrogenation is usually performed in the temperature range of 150° to 300°C over supported Pd catalysts (5–9), and different supports have been used, including alumina, that may act as Lewis acids (9). The gas-phase process can be carried out easily in continuous reactors for higher throughput. Liquid-phase phenol hydrogenation offers cost and energy savings, because the reaction can be performed at relatively low temperatures (10–15). Many researchers have contributed to this area, and multiple catalysts have been screened, such as Rh/C (10), Rh/C nanofiber (11), Pd/hydrophilic C (12), Ru/poly(*N*-vinyl-2-pyrrolidone) (PVP) (13), Pd/Mg and Pd/Fe (14), mesoporous Ce-doped Pd (15), and Pd/C (16). However, the attainment of high selectivity (>95%) at elevated conversion (>80%) with a satisfactory rate is a great challenge (8, 17), because the cyclohexanone product can be further hydrogenated to cyclohexanol under the reaction conditions (7, 15).

We report here that Pd/C, Pd/Al₂O₃, and Pd/NaY zeolite (18) (NaY zeolite is hereafter denoted NaY) catalysts and solid Lewis acids show excellent synergy in the hydrogenation of phenol to cyclohexanone, together substantially enhancing both activity and selectivity. The reaction can be carried out effectively at temperatures as low as 30°C, and >99.9% conversion of phenol is observed with >99.9% selectivity to cyclohexanone. Separation of the product from the catalyst–Lewis acid system is simple, and the catalyst system can be reused directly. This route has great potential for industrial application.

Our experiments (18) showed that dichloromethane is the best reaction solvent among several tested (table S2). Table 1 presents the results of phenol hydrogenation under different conditions over Pd/C, Pd/Al₂O₃, and Pd/NaY catalysts with and without AlCl₃. The conversion of phenol was very low, and considerable byproduct was produced when only the Pd/C catalyst was used (Table 1, entry 1), and the reaction did not occur at all when only Lewis acid (AlCl₃) was used (Table 1, entry 2). When Pd/C and AlCl₃ were used at the same time, the reaction proceeded with a selectivity of >99.9% up to complete conversion at 1.0 MPa of H₂ and a temperature at or below 50°C (Table 1, entries 3 to 5). At higher temperature, the reaction reached completion in 1 hour and the selectivity remained >99% (Table 1, entries 9 and 10). With other conditions fixed, an increase in hydrogen pressure (Table 1, entries 6 to 12) shortened the time to completion but slightly reduced the selectivity to cyclohexanone. Other Lewis acids were also effective in promoting the reaction [Table 1, entries 13 to 18; see also fig. S7 and supporting online material (SOM) text]. The activity and selectivity of the reaction using Pd/Al₂O₃ and Pd/NaY (18) were also enhanced effectively by AlCl₃ (Table 1, entries 19 to 26). The prospects for recycling Pd/C–ZnCl₂ were tested (18), and the results indicated that the catalyst system could

Beijing National Laboratory for Molecular Sciences, Institute of Chemistry, Chinese Academy of Sciences, Beijing 100190, China.

*To whom correspondence should be addressed. E-mail: Jiangt@iccas.ac.cn (T.J.); Hanbx@iccas.ac.cn (B.H.)